Calculation of positron binding energies of amino acids with the any-particle molecular-orbital approach

J. Charry,[1] J. Romero,[1] M. T. do N. Varella,[2] and A. Reyes[1]
[1]*Department of Chemistry, Universidad Nacional de Colombia, Bogotá, Cundinamarca 111321, Colombia*
[2]*Instituto de Física, Universidade de São Paulo, CP 66318, 05315-970 São Paulo, São Paulo, Brazil*
(Received 21 November 2013; published 14 May 2014)

We report positron binding energies (PBEs) for the 20 standard amino acids in the global minimum, hydrogen-bonded, and zwitterionic forms. The calculations are performed at the any-particle molecular-orbital (APMO) Hartree-Fock (HF), Koopmans' theorem (KT), second-order Möller-Plesset (MP2), and second-order propagator (P2) levels of theory. Our study reveals that the APMO KT and APMO P2 methods generally provide higher PBEs than the APMO HF and APMO MP2 methods, respectively, with only a fraction of the computational costs of the latter. We also discuss the impact of the choice of the positronic center on the PBEs and propose a simple and inexpensive procedure, based on the condensed Fukui functions of the parent molecules, to select the most suitable expansion center. The results reported so far indicate that APMO KT and APMO P2 methods are convenient options for a qualitative or semiquantitative analysis of positron binding in medium to large polyatomic systems.

DOI: 10.1103/PhysRevA.89.052709 PACS number(s): 34.80.Lx, 36.10.−k

I. INTRODUCTION

The past few decades have witnessed an increasing interest in the physics and chemistry of positronic systems in the low-energy regime [1–3]. Major advances in techniques for accumulating and manipulating positrons [2] have given rise to fascinating applications such as the production of antihydrogen [4], positronium (Ps) molecules [5], the scattering of slow Ps atoms [6,7], and energy-resolved annihilation measurements [3]. In the latter case, vibrational resonances leading to very high annihilation rates have unveiled a very rich physics underlying the formation of positronic molecules. As the mechanisms for resonantly enhanced positron annihilation involve the formation of bound positronic molecules, the positron binding energies (PBEs) can be obtained from the red shifts of the vibrational Feshbach resonances with respect to the vibrational spectra of the isolated molecules [1,2,8]. Accurate theoretical estimations of these bound states are thus invaluable tools to better understand resonant annihilation mechanisms.

In recent years there have been significant efforts to develop theoretical methods to calculate PBEs. Perhaps the most important conclusion of these studies would be the crucial contribution from the electron-positron (e-p) dynamical correlation to positron binding. Explicitly correlated Gaussian methodologies [9–13], Monte Carlo methods [14–16], and full configuration-interaction methods [17,18] have demonstrated superior performance in the description of e-p correlation and estimation of PBEs. Despite their proven accuracy, these approaches are extremely computationally demanding and calculations are only feasible for studying relatively small systems, namely, atoms [19–24], diatomic molecules [23,25–28], and linear triatomics [19,29]. A notable exception would be the positron-formaldehyde study by Strasburger [30]. The more accurate though more demanding multicomponent quantum Monte Carlo method has also been applied to hydrogen cyanide by Kita *et al.* [31].

Since most experiments have addressed larger molecules of chemical and biological interest, it is desirable to develop computationally viable theoretical approaches that can be used to study these polyatomic positronic systems, at least in a qualitative or semiquantitative manner. Efforts in this direction have been conducted by Tachikawa and co-workers. They have calculated positron binding energies for several polyatomic molecules [27,32–37] by employing the multicomponent molecular-orbital (MCMO) approach at the Hartree-Fock (HF) level. Although this method usually underestimates the binding energies with respect to the experimental data or high-level calculations [3], it provides a fair qualitative description of PBEs at a reasonable numerical effort, thus allowing for applications to a variety of polyatomic systems.

In view of the facts outlined above, the application of alternative theoretical and computational tools to address positronic molecules is desirable. To this aim, in this work we employ the any-particle molecular-orbital (APMO) method [38] to calculate the PBEs of the 20 standard amino acids. The APMO method is a multicomponent wave-function approach to study systems containing any type and number of quantum species, such as muonic atoms [39,40] or molecules containing quantum electrons and quantum nuclei [38,41–46]. Our motivation to study amino acids in this application of the APMO method to positronic systems is twofold. First, there is an increasing interest in positron interactions with biomolecules [47–49], motivated by possible applications in cancer therapy [50], positron emission tomography [51], and mass spectrometry [52,53]. Second, PBEs for the 20 standard amino acids, in both the global minimum (GM) and hydrogen-bonded (HB) conformations, were recently obtained with the MCMO HF method [36].

In the present study, we consider the neutral GM and HB conformations and also the zwitterionic (ZW) isomers. We employ the uncorrelated APMO HF method, which is similar to the MCMO HF approach, as well as different approximations to the e-p correlation energy within the APMO framework, namely, the second-order Möller-Plesset (MP2) perturbation theory [54] and the generalized second-order propagator (P2) theory [44,55]. We discuss the contribution

from the e-p correlation to the binding energies, as obtained from the APMO MP2 and APMO P2 calculations, and we also propose a simple scheme, based on the condensed Fukui functions [56], to select the most suitable center to expand the positron orbital.

This paper is organized as follows. In Sec. II we summarize the equations of the APMO HF, APMO MP2, and APMO P2 methods. In Sec. III we describe the procedure to choose the center of the positron basis set and describe how the PBEs are calculated in each level of theory. In Sec. IV we compare the PBEs obtained with different positron basis-set centers and with the different theories, for the whole set of GM and HB conformers and ZW isomers. A summary and perspectives for future work are given in Sec. V.

II. THEORY

This section summarizes the working equations of the APMO HF, APMO MP2, and APMO P2 levels of theory, as applied to molecular systems containing multiple electrons and one positron.

A. The APMO HF theory

In the framework of the Born-Oppenheimer approximation, the molecular Hamiltonian H (in atomic units) of a system comprised of N^{e^-} quantum electrons e^-, a single positron e^+, and N^C classical point-charge nuclei can be written as

$$H = \sum_i^{N^{e^-}} -\left[\frac{1}{2}\nabla_i^2 + \sum_p^{N^C}\frac{Q^p}{r_{ip}}\right] + \left[-\frac{1}{2}\nabla_k^2 + \sum_p^{N^C}\frac{Q^p}{r_{kp}}\right] + \sum_i^{N^e}\sum_{j>i}^{N^e}\frac{1}{r_{ij}} - \sum_i^{N^e}\frac{1}{r_{ik}} + \sum_p^{N^C}\sum_{q>p}^{N^C}\frac{Q^pQ^q}{r_{pq}}. \quad (1)$$

Here i and j, k, and p and q are indices for the electrons, the positron, and the nuclei, respectively, while Q^p and Q^q are the nuclear charges. The APMO HF level wave function for this molecular system Ψ_0 is constructed as a product of a single-configurational electronic wave function Φ^{e^-} and a spin orbital for the single positron Φ^{e^+},

$$\Psi_0 = \Phi^{e^-}\Phi^{e^+}, \quad (2)$$

where Φ^{e^-} and Φ^{e^+} are built from molecular orbitals ψ_i^α, which are obtained by solving the Fock equations given by

$$f^\alpha(i)\psi_i^\alpha = \varepsilon_i^\alpha\psi_i^\alpha, \quad \alpha = e^-, e^+, \quad (3)$$

where the effective one-particle Fock operators $f^\alpha(i)$ for quantum species e^- and e^+ are expanded as

$$f^{e^-}(i) = h^{e^-}(i) + \sum_j^{N^{e^-}}\left[J_j^{e^-} - K_j^{e^-}\right] - J^{e^+}, \quad (4)$$

$$f^{e^+}(i) = h^{e^+}(i) - \sum_j^{N^{e^-}} J_j^{e^-}. \quad (5)$$

In the above equations $h^\alpha(i)$ is the single-particle core Hamiltonian

$$h^\alpha(i) = -\frac{1}{2}\nabla_i^2 + \sum_p^{N^C}\frac{Q^pQ^\alpha}{r_{ip}} \quad (6)$$

and J^α and K^α are Coulomb and exchange operators defined as

$$J_j^\alpha(1)\psi_i^\beta(1) = Q^\alpha Q^\beta\left[\int d\mathbf{r}_2\psi_j^{\alpha*}(2)\frac{1}{r_{12}}\psi_j^\alpha(2)\right]\psi_i^\beta(1), \quad (7)$$

$$K_j^{e^-}(1)\psi_i^{e^-}(1) = \left[\int d\mathbf{r}_2\psi_j^{e^-*}(2)\frac{1}{r_{12}}\psi_i^{e^-}(2)\right]\psi_j^{e^-}(1) \quad (8)$$

for $\alpha,\beta = e^-, e^+$.

B. The APMO MP2 theory

The APMO MP2 energy of a molecular system containing N^{e^-} electrons and one positron is given by [54]

$$E^{\text{APMO MP2}} = E^{(0)} + E^{(2)}_{e^-e^-} + E^{(2)}_{e^-e^+}, \quad (9)$$

where $E^{(0)}$ is the APMO HF energy, while $E^{(2)}_{e^-e^-}$ and $E^{(2)}_{e^-e^+}$ are the second-order electron and electron-positron correlation energies, respectively. Here $E^{(2)}_{e^-e^-}$ is written in the physicist notation [57,58] of quantum chemistry as

$$E^{(2)}_{e^-e^-} = \frac{1}{4}\sum_{a^{e^-}}^{O^{e^-}}\sum_{b^{e^-}}^{O^{e^-}}\sum_{r^{e^-}}^{V^{e^-}}\sum_{s^{e^-}}^{V^{e^-}} \times \frac{|\langle a^{e^-}b^{e^-}|r^{e^-}s^{e^-}\rangle - \langle a^{e^-}b^{e^-}|s^{e^-}r^{e^-}\rangle|^2}{\epsilon_a^{e^-} + \epsilon_b^{e^-} - \epsilon_r^{e^-} - \epsilon_s^{e^-}}, \quad (10)$$

where O^{e^-} and V^{e^-} are, respectively, the number of occupied and virtual electronic orbitals such that a^{e^-} and b^{e^-} run over the occupied electronic orbitals, while r^{e^-} and s^{e^-} over the virtual electronic orbitals. The second-order electron-positron correlation term for a positron in the ground-state orbital a^{e^+} is

$$E^{(2)}_{e^-e^+} = \sum_{a^{e^+}}^{O^{e^+}}\sum_{a^{e^-}}^{O^{e^-}}\sum_{r^{e^+}}^{V^{e^+}}\sum_{r^{e^-}}^{V^{e^-}}\frac{|\langle a^{e^+}a^{e^-}|r^{e^+}r^{e^-}\rangle|^2}{\epsilon_a^{e^+} + \epsilon_a^{e^-} - \epsilon_r^{e^+} - \epsilon_r^{e^-}}, \quad (11)$$

where $a^{e^\pm}$ and $r^{e^\pm}$ are occupied and virtual orbitals, respectively. The second-order correction to the APMO HF energy has contributions from double electronic excitations, according to Eq. (10), and from double excitations comprising single excitations of the electronic and positronic subspaces, as given in Eq. (11). Both the direct rs and exchange sr contributions are accounted for in Eq. (10) and the MP2 perturbation potential, namely, the difference between the sum of the Coulomb interactions and the sum of the single-particle Fock potentials [57], is implied in the above expressions.

C. The APMO P2 theory

Here we summarize the expressions of the second-order generalized propagator (APMO P2) for molecular systems comprising multiple electrons and one positron. A general formulation of the method can be found elsewhere [44]. At the APMO HF level of theory, the energy of the pth occupied

positron orbital $\varepsilon_p^{e^+}$ can be obtained by solving Eq. (5). This energy provides a first estimate of the PBE,

$$-\mathrm{PBE}^{\mathrm{KT}} = \varepsilon_p^{e^+}, \tag{12}$$

which is equivalent to the Koopmans' theorem (KT) approximation for the electron binding energies. In the framework of APMO propagator theory [44], the KT approximation in Eq. (12) can be improved with the inclusion of the relaxation and correlation corrections, via the self–energy term $\Sigma_{pp}^{e^+}(\omega_p^{e^+})$, such that

$$-\mathrm{PBE}^{\mathrm{P2}} = \omega_p^{e^+}, \tag{13}$$

where $\omega_p^{e^+}$ is the optimized orbital energy for pth orbital obtained by solving the following equation iteratively:

$$\omega_p^{e^+} = \varepsilon_p^{e^+} + \Sigma_{pp}^{e^+}\left(\omega_p^{e^+}\right), \tag{14}$$

with

$$\begin{aligned}\Sigma_{pp}^{e^+}\left(\omega_p^{e^+}\right) &= \Sigma_{pp}^{e^+e^-(2)}\left(\omega_p^{e^+}\right)\\ &= \sum_{a^{e^-}}^{O^{e^-}}\sum_{r^{e^-}}^{V^{e^-}}\sum_{r^{e^+}}^{V^{e^+}}\frac{|\langle p^{e^+}a^{e^-}|r^{e^+}r^{e^-}\rangle|^2}{\omega_p^{e^+}+\epsilon_a^{e^+}-\epsilon_r^{e^-}-\epsilon_r^{e^+}}\\ &+ \sum_{a^{e^-}}^{O^{e^-}}\sum_{r^{e^-}}^{V^{e^-}}\sum_{a^{e^+}}^{O^{e^+}}\frac{|\langle p^{e^+}r^{e^-}|a^{e^+}a^{e^-}\rangle|^2}{\omega_p^{e^+}+\epsilon_r^{e^-}-\epsilon_a^{e^+}-\epsilon_a^{e^-}}\end{aligned} \tag{15}$$

where $a^{e^\pm}$ and $r^{e^\pm}$ are occupied and virtual orbitals, respectively.

III. COMPUTATIONAL ASPECTS

The GM and HB structures of the 20 amino acids (isolated molecules) were optimized at the HF level of theory with the 6-311++G(d,p) electronic basis set. The ZW structures, unstable in the gas phase, were optimized at the same level of theory, though considering water as an implicit solvent within the polarizable continuum model (PCM) [59,60]. All optimization calculations were performed with the GAMESS package [61] and the same optimized geometries were used for the positronic complexes assuming that relaxation upon positron binding would be negligible, as pointed out in Ref. [36].

The APMO HF, APMO MP2, and APMO P2 calculations for the amino-acid–positron systems were carried out with the LOWDIN code [46] considering the electrons and the positron as quantum particles in gas phase. The calculations were performed with the 6-311++G(d,p)/11s11p11d electron-positron basis sets. The latter was generated with an even-tempered scheme $\alpha_{i+1} = b \times \alpha_i$, with $\alpha_0 = 1 \times 10^{-3}$ and $b = 3.000$ for s-, p-, and d-type Gaussian functions [36].

The condensed Fukui functions f_k^- of a molecule with N electrons are calculated as [56]

$$f_k^- = q_k(N-1) - q_k(N), \tag{16}$$

where $q_k(N-1)$ and $q_k(N)$ are the electronic populations of the kth atom in the cationic $(N-1)$-electron system and the neutral N-electron system. At the APMO HF and APMO MP2 levels of theory, the PBEs $\mathcal{E}_{\mathrm{PBE}}$ are obtained as the difference between the energies of the amino acid X and the corresponding positronic complex e^+X,

$$\mathcal{E}_{\mathrm{PBE}}^{\mathrm{HF,MP2}} = E^{\text{APMO HF,APMO MP2}}[X] - E^{\text{APMO HF,APMO MP2}}[e^+X], \tag{17}$$

while APMO KT and APMO P2 PBEs are calculated employing Eqs. (12) and (14) for the corresponding e^+X complex.

IV. RESULTS AND DISCUSSION

A. Positron basis-set center

Ideally, there should be several expansion centers for positronic basis sets around the molecular region. While this procedure would be expected to offer a better prediction of the PBE, it would be impractical for medium- to large-size molecules. Fortunately, previous studies on polar molecules have shown that the weakly bound positron occupies a diffuse orbital around the negative end of the molecular dipole moment [27,33,35,36]. Therefore, reasonable PBE estimates can still be obtained with a single basis-set center, as long as the basis set and the expansion center are suitably chosen. Electron and positron basis sets should contain enough polarization and diffuse functions to account for the polarization and dispersion stabilization of the molecule upon positron binding. The center of the positron basis set should in turn be chosen on the basis of some optimization criterion, for instance, maximizing the PBE.

We propose a simple and computationally inexpensive procedure to choose the positron basis-set center based on the condensed Fukui functions f^-, given in Eq. (16). Since positive values of these functions are associated with the ability of an atom in a molecule to attract positive charges [56], we place the positron basis set on the atom with the largest value of f^- in the neutral molecule. In view of the variational nature of the APMO HF theory, improving the basis sets should lower the total energy of the positronic molecule. One could thus expect that locating the positron basis set on the atom with the largest value of the Fukui function should give rise to the lowest total energy. To verify this assumption, we carried out a series of APMO HF single-point calculations for glycine, placing the positron basis set on each of the atoms in the GM, HB, and ZW conformations. The results are shown in Table I, where the f^- values were obtained with Mulliken atomic charges [57] and atomic charges from electrostatic potentials using a grid-based method (CHELPG) [62].

The APMO HF total energies, given as deviations from the lowest value $\Delta E = E_{\mathrm{HF}} - E_{\mathrm{HF}}^{\mathrm{min}}$, are nearly insensitive to the choice of expansion center for the GM form, as the energy variations do not exceed 0.04 meV, consistent with the calculations of Ref. [36]. In contrast, the positron basis-set center significantly impacts the total energies of the HB and ZW structures, with ΔE ranging from 2.9 to 30 meV and from 14.5 to 270 meV, respectively. In all cases, the largest value of the Fukui function of the neutral molecule gives rise to the lowest total energy of the positronic system, in agreement with the argument given above. The PBEs obtained with the APMO HF scheme show the same behavior. The binding energy of the GM form does not vary as the positron basis set is placed on the different atoms, whereas large deviations are obtained

TABLE I. Condensed Fukui function f_k^- for the atoms of glycine at the GM, HB, and ZW structures. The APMO HF total energies of the positronic molecules were obtained by placing the positronic basis set on each atom and the results are given as deviations from the lowest value $\Delta E = E_{\rm HF} - E_{\rm HF}^{\rm min}$. The PBEs were calculated with the APMO HF method using expression (17). Marked in bold are the highest positive value of the condensed Fukui function, the lowest total energy, and also the highest PBE. The $f^-(a)$ are from Mulliken atomic charges and the $f^-(b)$ are from CHELPG atomic charges.

		GM				HB				ZW			
No.	Atom	$f^-(a)$	$f^-(b)$	ΔE (meV)	PBE (meV)	$f^-(a)$	$f^-(b)$	ΔE (meV)	PBE (meV)	$f^-(a)$	$f^-(b)$	ΔE (meV)	PBE (meV)
1	C	0.05	−0.04	0.01	−1.8	0.01	−0.09	2.90	54.4	−0.09	−0.19	14.51	548.1
2	C	−0.17	−0.48	0.02	−1.8	0.00	−0.14	13.68	43.7	0.04	−0.01	108.99	453.7
3	N	**0.54**	**1.17**	**0.00**	−1.8	0.02	0.04	23.93	33.4	0.00	−0.14	218.87	343.8
4	O	0.09	0.11	0.01	−1.8	0.10	0.22	9.23	48.1	0.20	0.29	61.34	501.3
5	O	0.03	0.15	0.04	−1.8	**0.59**	**0.64**	**0.00**	**57.3**	**0.64**	**0.69**	**0.00**	**562.6**
6	H	0.10	0.14	0.02	−1.8	0.05	0.11	18.53	38.8	0.06	0.07	168.38	394.3
7	H	0.10	0.14	0.02	−1.8	0.08	0.10	18.94	38.4	0.06	0.07	169.48	393.2
8	H	0.11	−0.09	0.00	−1.7	0.04	0.04	26.76	30.6	0.02	0.06	229.78	332.9
9	H	0.11	−0.09	0.00	−1.7	0.05	0.06	28.74	28.6	0.02	0.06	234.47	328.2
10	H	0.04	0.00	0.04	−1.8	0.05	0.02	17.60	39.7	0.05	0.10	269.30	293.3

for the HB and ZW isomers, with the largest PBE arising from the largest value of f^-.

B. Structures and dipole moments

The dipole moments were calculated at the optimized gemeotries, as described in Sec. III. Figure 1 shows the structures of the glycine isomers, while the structures of the other amino acids are provided in Ref. [59].

The ZW isomers were considered in the present study in view of their biological relevance, as they are the most stable forms in aqueous solution. In addition, the deprotonation of the carboxyl group gives rise to a full −1 charge that strongly favors the interaction between the positron and the –COO^- moiety. Local effects, around the carboxylate group, could thus take place in the positronic molecules built on ZW structures, while the positron interaction with the dipole moment potential would be expected to prevail in the GM and HB forms. Therefore, a comparison of the ZW positronic molecules with their GM and HB counterparts would be very interesting in terms of positron binding and *e-p* correlation. Since the isolated ZW molecules do not have stable geometries, the optimization was carried out in solution, within the PCM framework, and the isolated and positronic ZW systems were considered at these geometries. This procedure not only circumvents difficulties related to the description of the positron-solvent interaction, but also allows for a meaningful comparison between the PBEs of the ZW forms and those of the GM and HB forms in the gas phase.

Table II shows the calculated dipole moments of the amino acids in the GM, HB, and ZW structures. The average dipole moment magnitudes of the HB and ZW isomers are, respectively, three and six times as large as those of the GM structures. Histidine would be the only exception, since it is more strongly polar in the GM conformation (4.89 D) than in the HB conformation (3.13 D). According to the well-known fixed-dipole model [63], dipole-supported bound states should exist for $\mu > 1.625$ D, with a direct correlation between the binding energies and the dipole moment magnitudes, such that one would expect the trend that the ZW PBE is greater than the HB PBE, which is greater than the GM PBE. Table II also shows the dipole moments reported by Koyanagi *et al.* [36], obtained at the MCMO HF 6-31*G theory level, for the GM and HB structures. Even though the overall agreement between our results and those Koyanagi *et al.* is fairly good, the observed small deviations are associated with the use of different basis sets and optimized geometries.

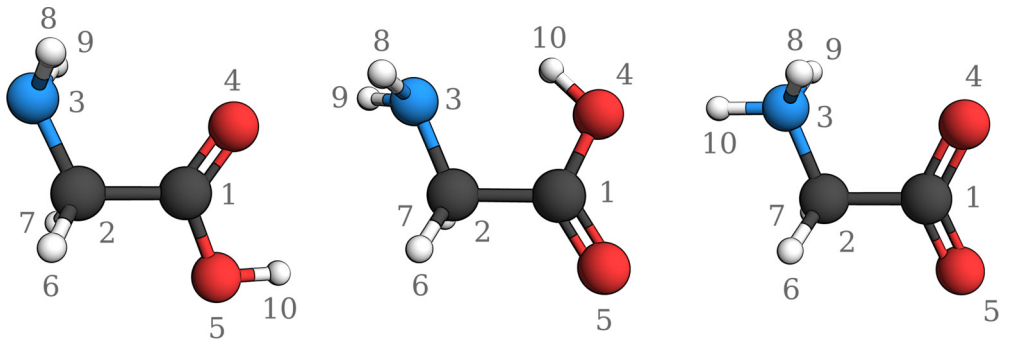

FIG. 1. (Color online) The HF 6-311++G(d,p) optimized structures of glycine: global minimum (left), hydrogen bonded (middle), and zwitterion (right).

TABLE II. Molecular dipole moments obtained at the HF 6-311++G(d,p) level for the standard amino acids in the GM, intramolecular HB, and ZW conformations. The HF 6-31*G results of Ref. [36] are given in parentheses for comparison.

	μ (D)		
Amino acid	GM	HB	ZW
Ala	1.43 (1.40)	5.60 (5.50)	11.93
Arg	2.90 (2.25)	7.40 (6.96)	14.24
Asn	2.62 (2.93)	4.69 (4.64)	10.16
Asp	1.55 (2.28)	4.54 (4.57)	10.74
Cys	1.76 (1.99)	4.13 (4.12)	10.30
Gln	3.61 (3.44)	6.28 (6.44)	14.42
Glu	2.12 (1.89)	6.55 (6.54)	12.85
Gly	1.30 (1.33)	5.76 (5.69)	12.52
His	4.89 (3.91)	3.13 (4.19)	8.78
Ile	1.43 (1.36)	5.48 (5.43)	11.39
Leu	1.26 (1.20)	5.74 (5.62)	11.90
Lys	1.89 (2.43)	4.40 (5.92)	10.56
Met	2.20 (1.84)	4.45 (6.63)	10.69
Phe	1.31 (1.32)	5.61 (5.71)	11.92
Pro	1.85 (1.64)	6.03 (5.85)	12.37
Ser	2.88 (1.96)	4.31 (4.53)	12.50
Thr	2.75 (2.28)	4.43 (3.73)	10.31
Trp	1.19 (4.18)	7.08 (6.40)	13.33
Tyr	2.69 (2.63)	4.97 (3.73)	11.43
Val	1.40 (1.40)	5.31 (5.21)	11.42

In addition, Fig. 2 displays the positronic and electronic densities for the HB and ZW forms of glycine. It can be clearly seen that the positronic density gradually localizes around the negative region of the dipole as it increases its magnitude.

C. Positron binding energies

Positron binding energies calculated with the MCMO HF method are usually underestimated [36,64], due to the lack of dynamical e-p correlation. Despite this limitation, these PBE estimates are useful for (i) a qualitative understanding of positronic systems and (ii) establishing lower bounds for the PBEs and hence the cost-benefit relation for the higher-level methods [3]. As mentioned in the Introduction, while several potentially accurate methods are available, e.g., the quantum Monte Carlo and explicitly correlated techniques, their applications are generally restricted to atoms and small molecules, in view of their extremely high computational effort.

To proceed beyond the HF level without running into computer limitations in the present work we improve the APMO HF results with e-p correlation estimates obtained at the APMO MP2 and APMO P2 levels. The results for the 60 structures, namely, the GM and HB conformers and ZW isomers of the 20 standard amino acids, are summarized in Table III, along with the MCMO HF results of Ref. [36] for the GM and HB structures. Also, Fig. 3 plots our APMO HF PBE results for the GM and HB structures and contrast them with those of the Koyanagi *et al.* [36]. The major source of differences in the PBEs reported in Fig. 3 is the use of two very distinct electronic-positronic basis sets 6-31G(d):11s9p4d2f1g and 6-311++G(d,p):11s11p11d as well the use of different optimized geometries for these calculations.

In general, the HB and ZW forms are capable of binding the positron, as indicated by their positive PBE values, even at the APMO HF level. In contrast, the GM structures do not give rise to bound positronic molecules, except for the APMO P2 results for Gln, His, and Ser. Although generally higher with respect to the APMO HF calculations, the PBE estimates obtained from the APMO MP2 and APMO P2 methods are still expected to provide lower bounds such that one should not conclude that the GM structures are not able to bind positrons, based only on the present calculations. Nevertheless, the results in Table III indicate significant contributions from the e-p correlation to the binding energies, even for the strongly polar molecules. For the HB structures, there is an average increase in the PBE magnitude of 39.1% (APMO MP2 level) and 105.0% (APMO P2 level) with respect to the APMO HF results. Even for the ZW structures, having dipole moment magnitudes around 10 D, the average PBEs are increased by 17.7% and 20.6% in the APMO MP2 and APMO P2 calculations, respectively. Finally, the APMO KT estimates of the binding energies, obtained from Eq. (12), are also generally higher with respect to the APMO HF binding energies, calculated as the difference between the total energies of the positronic and isolated molecules. For the

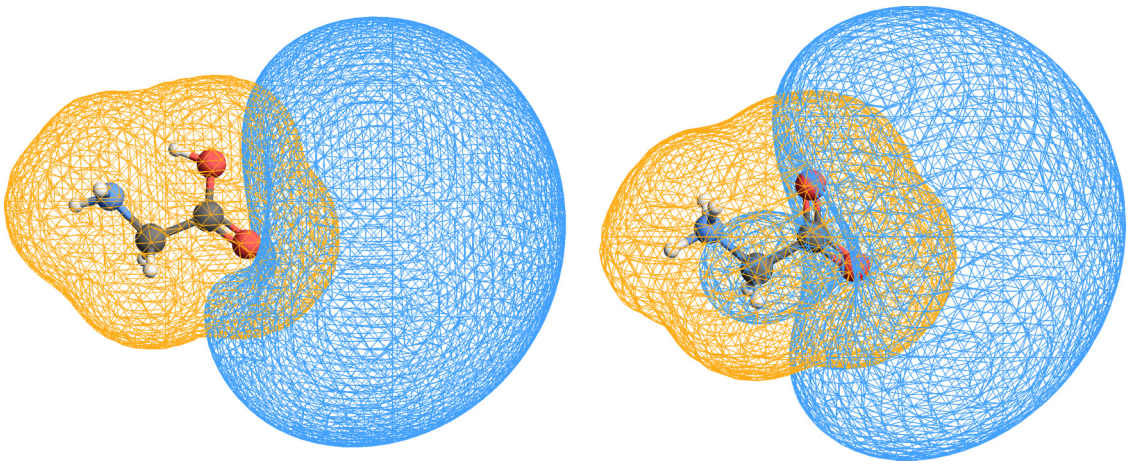

FIG. 2. (Color online) Electronic density (orange) and positronic density (blue) for the hydrogen-bonded (left) and zwitterionic (right) conformations of the glycine e^+ system. The contour value of 0.0001 was used for all densities.

TABLE III. APMO HF, APMO KT, APMO MP2, and APMO P2 calculated PBEs for the standard amino acids at the GM, HB, and ZW structures. Calculations were performed with the 6-311++G(d,p)/11s11p11d electron-positron basis sets. Amino acids are denoted by their three-letter abbreviations. For contrast, the MCMO HF 6-31*G results from Koyanagi *et al.* for GM and HB conformations are reported in parentheses [36].

	GM PBE (meV)				HB PBE (meV)				ZW PBE (meV)			
Amino acid	HF	KT	MP2	P2	HF	KT	MP2	P2	HF	KT	MP2	P2
Ala	−1.7	−1.7	−1.7	−1.6	52.9 (47.8)	64.3	68.1	103.2	531.7	620.2	617.4	752.0
Arg	−0.8	−0.8	−0.9	−0.4	70.6 (78.5)	87.3	89.3	129.3	565.2	670.4	652.9	799.9
Asn	−0.6	−0.6	−0.6	−0.2	16.9 (17.6)	20.4	29.4	39.7	475.1	564.4	583.5	690.9
Asp	−1.7	−1.7	−1.7	−1.6	18.0 (19.3)	21.8	29.4	41.4	448.8	532.2	548.3	653.2
Cys	−1.6	−1.6	−1.4	−1.5	14.8 (14.0)	18.7	24.1	38.1	436.5	524.4	525.0	642.9
Gln	0.9 (1.9)	1.0	0.4	2.3	47.8 (54.4)	58.3	66.8	93.2	591.7	696.1	682.2	827.7
Glu	−1.4	−1.3	−1.5	−1.1	62.8 (66.4)	76.6	79.4	115.4	529.4	625.4	621.0	752.3
Gly	−1.8	−1.8	−1.7	−1.7	57.3 (55.1)	67.8	70.2	105.5	562.6	643.9	641.1	777.3
His	4.8 (14.9)	5.1	7.3	7.0	3.1 (9.5)	4.2	5.5	13.3	412.7	507.5	490.0	624.0
Ile	−1.7	−1.7	−1.7	−1.6	48.7 (47.8)	63.1	69.4	104.2	500.1	606.5	596.4	736.1
Leu	−1.8	−1.8	−1.8	−1.7	58.1 (55.2)	73.9	79.6	117.2	555.4	662.1	650.4	795.6
Lys	−1.6	−1.6	−1.5	−1.5	36.3 (57.4)	48.5	53.5	84.8	518.6	622.0	611.9	752.7
Met	−1.4	−1.4	−1.3	−1.2	30.1 (62.0)	39.7	48.0	72.0	510.3	613.4	608.5	741.1
Phe	−1.8	−1.8	−1.8	−1.7	50.6 (54.1)	67.6	72.8	107.5	536.4	650.7	633.2	776.3
Pro	−1.5	−1.5	−1.4	−1.2	72.0 (67.0)	90.4	94.8	138.4	573.8	678.5	659.1	813.8
Ser	−0.2	−0.2	−0.2	0.8	9.3 (23.9)	10.7	12.3	21.6	589.4	681.9	676.1	818.1
Thr	−0.8	−0.8	−0.7	−0.4	11.5 (28.5)	13.5	16.0	27.0	379.9	453.9	453.5	564.7
Trp	−1.8 (4.0)	−1.8	−1.8	−1.7	79.4 (70.7)	105.1	113.8	153.4	597.0	723.2	709.0	851.6
Tyr	−1.1	−1.1	−1.0	−0.9	41.0 (13.8)	55.6	63.6	91.9	542.8	659.1	646.5	785.6
Val	−1.7	−1.7	−1.7	−1.6	42.3 (36.7)	53.9	60.0	91.3	501.2	603.8	594.5	733.8
average					41.2	52.1	57.3	84.4	517.7	617.0	609.8	744.5

HB conformers and ZW isomers, the average APMO KT binding energies are increased by 26.4% and 19.1%, respectively.

D. Positron binding energies and dipole moments

Since the fixed-dipole model [63] predicts that molecules with critical dipole moment magnitudes ($\mu > 1.625$ D) could bind a positron (or an electron), one would expect some correlation between the dipole moments and the PBEs. From the available PBE experimental data [3,8], a linear scaling of the PBE with respect to both the dipole moment magnitude and the average polarizability has been proposed and the previously reported PBE estimates for the amino acids (GB and HB structures) computed at the MCMO HF 6-31*G level [36] indeed show a linear behavior with respect to the dipole moments.

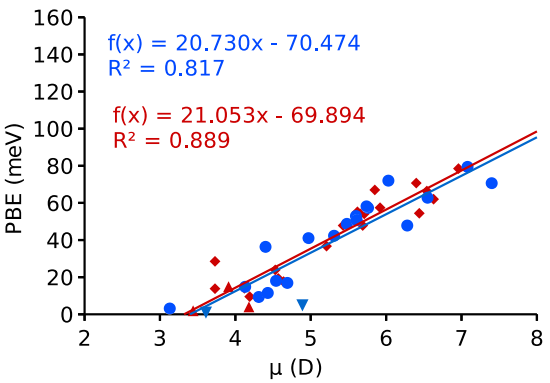

FIG. 3. (Color online) Positron binding energies and molecular dipole moments μ at the Hartree-Fock level of theory. The results of Koyanagi *et al.* are in red and our results are in blue. Circles and rhombi depict hydrogen-bonded structure data and triangles global minimum structure data.

Figure 3 plots our APMO HF PBE results for the GM and HB structures and contrast them with those of Koyanagi *et al.* [36]. The major source of differences in the PBEs reported in Fig. 3 is the use of two very distinct electronic-positronic basis sets, namely, 6-31G(d):11s9p4d2f1g and 6-311++G(d,p):11s11p11d, which gives rise to slight differences in geometry and dipole moment magnitudes.

Figure 4 plots the presently calculated PBEs against the dipole moment magnitudes for the HB conformers and ZW isomers. The results for the GM structures were not included since most of the species do not form stable positronic complexes. For the HB structures, the correlation coefficients R^2 obtained from linear regressions were 0.842, 0.814, 0.803, and 0.773 for the APMO HF, APMO KT, APMO MP2, and APMO P2 computations, respectively. The larger deviation from the linear behavior in the higher-level calculations is not surprising. At the APMO HF level, the dipole interaction would be expected to drive the binding process, due to the lack of e-p correlation. As the latter effect is partially included in the APMO MP2 and APMO P2 calculations, the resulting PBEs become less correlated with the dipole moment magnitudes. This is particularly evident for the HB structures with dipole moments around 4–5 D since the vertical spreading of the data significantly increases as the theory level is improved from APMO HF to APMO P2.

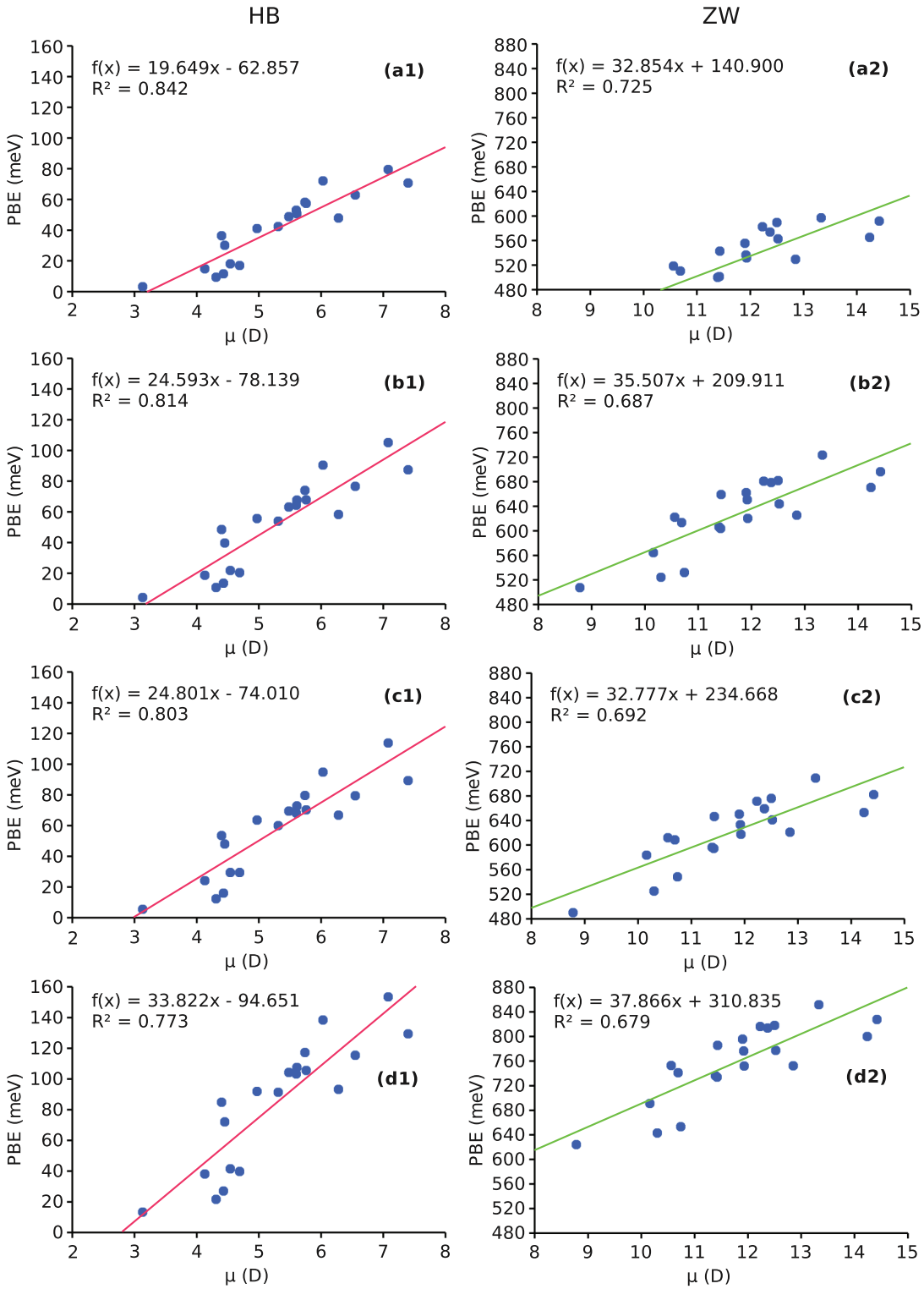

FIG. 4. (Color online) Positron binding energies against the molecular dipole moments μ. The circles indicate the present calculations and the straight lines are linear regressions. The results obtained with the (a) APMO HF, (b) APMO KT, (c) APMO MP2, and (d) APMO P2 methods are depicted, respectively, for the (1) HB structures and (2) ZW structures.

Critical dipole moment magnitudes can also be inferred from the extrapolation of the linear regressions to $\mathcal{E}_{\mathrm{PBE}} = 0$. For the HB structures we obtained 3.20, 3.18, 2.98, and 2.80 D for the APMO HF, APMO KT, APMO MP2, and APMO P2 calculations, respectively. The prediction of the fixed dipole model ($\mu_{\mathrm{crit}} = 1.625$ D) is known to significantly underestimate the critical dipole moment magnitude of actual molecules. It has been pointed out that molecules with

$\mu \gtrsim 2.5$ D would bind an electron [65], while positron binding would be ensured for $\mu \gtrsim 3.6$ D [3], even though molecules with $\mu > 2.7$ D already show substantial binding energies [8]. The present estimates for the HB structures, $\mu_{\rm crit} \approx 3$ D, would thus be consistent with these observations and they also point out that e-p correlation does play a role in the APMO MP2 and APMO P2 estimates as the corresponding critical dipole moments are smaller than the APMO HF estimates.

For the ZW structures, also shown in Fig. 4, the regression coefficients were 0.725, 0.687, 0.692, and 0.679 for the APMO HF, APMO KT, APMO MP2, and APMO P2 calculations, respectively. While these results would seem unexpected, as the more strongly polar molecules show less correlation between the dipole moment magnitudes and the binding energies, the intramolecular proton transfer in the ZW forms gives rise to a full -1 charge on the carboxylate group $-COO^-$. It is thus possible that the high PBEs of the ZW isomers would mostly arise from the local interactions of the positron with the negatively charged carboxylate moiety, namely, virtual positronium formation, as opposed to the interaction with the dipole moment potential.

E. Origin of the differences in the calculation of the PBEs

To gain some further insight into the present results, it would be instructive to analyze the APMO MP2 and APMO P2 corrections to the APMO HF and APMO KT binding energies, respectively. In the first case, we observe that the APMO HF level PBE is given by

$$\mathcal{E}_{\rm PBE}^{\rm HF} = E_{e^-}^{(0)} - E_{e^-,e^+}^{(0)}, \tag{18}$$

where the subscripts denote the quantum species and the superscripts indicate the type of contribution, while the APMO MP2 binding energy is expressed as

$$\mathcal{E}_{\rm PBE}^{\rm MP2} = E_{e^-}^{\text{APMO MP2}} - E_{e^-,e^+}^{\text{APMO MP2}}, \tag{19}$$

$$\mathcal{E}_{\rm PBE}^{\rm MP2} = \left[E_{e^-}^{(0)} + E_{e^-}^{(2),e^-}\right] - \left[E_{e^-,e^+}^{(0)} + E_{e^-,e^+}^{(2),e^-} + E_{e^-,e^+}^{(2),e^-,e^+}\right] \tag{20}$$

$$= \left[E_{e^-}^{(0)} - E_{e^-,e^+}^{(0)}\right] + \left[E_{e^-}^{(2),e^-} - E_{e^-,e^+}^{(2),e^-}\right] - E_{e^-,e^+}^{(2),e^-,e^+} \tag{21}$$

$$= \mathcal{E}_{\rm PBE}^{\rm HF} + E_{\rm relax}^{(2),e^-} - E_{e^-,e^+}^{(2),e^-,e^+}. \tag{22}$$

The $\mathcal{E}_{\rm PBE}^{\rm MP2}$ correction to $\mathcal{E}_{\rm PBE}^{\rm HF}$ involves two terms, namely, $E_{\rm relax}^{(2),e^-}$ and $E_{e^-,e^+}^{(2),e^-,e^+}$. The first describes the change in the electron correlation energy arising from positron binding and the latter accounts for e-p correlation. The decomposition of the APMO MP2 binding energy according to the above expressions is given in Table IV for the HB and ZW structures. The $E_{\rm relax}^{(2),e^-}$ contribution reduces binding energies, on average, by 23.1 and 97.6 meV for the HB conformers and ZW isomers, respectively. The loss of electron correlation in molecules interacting with external potentials, e.g., fields or other molecules, is usually attributed to the increase in the average interelectronic separation [66]. We are led to conclude, based on the negative values of the $E_{e^-,e^+}^{(2),e^-,e^+}$ term, that the attractive e-p interaction increases the average interelectronic distance as the molecule attaches the positron, thus leading to electron correlation loss. In addition, the larger absolute values of $E_{\rm relax}^{(2),e^-}$ for the ZW structures, in comparison with the HB counterparts, clearly indicate a more effective distortion of the electron cloud in the ZW forms.

TABLE IV. Energy components (in meV) of Eq. (22) for amino acids in the HB and ZW forms.

	HB			ZW		
Amino acid	$\mathcal{E}_{\rm PBE}^{\rm HF}$	$E_{\rm relax}^{(2),e^-}$	$E_{e^-,e^+}^{(2),e^-,e^+}$	$\mathcal{E}_{\rm PBE}^{\rm HF}$	$E_{\rm relax}^{(2),e^-}$	$E_{e^-,e^+}^{(2),e^-,e^+}$
Ala	52.9	−30.5	−45.7	531.5	−101.0	−186.7
Arg	70.6	−33.8	−52.5	565.0	−107.2	−194.9
Asn	16.8	−8.7	−21.3	474.9	−72.6	−181.0
Asp	18.0	−10.3	−21.8	448.6	−72.8	−172.2
Cys	14.8	−12.6	−21.9	436.3	−85.2	−173.6
Gln	47.8	−22.3	−41.3	591.5	−106.8	−197.3
Glu	62.8	−31.1	−47.7	529.2	−95.5	−187.1
Gly	57.3	−30.6	−43.5	562.4	−103.0	−181.5
His	3.1	−7.3	−9.7	412.5	−98.0	−175.4
Ile	48.7	−29.6	−50.3	499.9	−101.8	−198.0
Leu	58.0	−31.9	−53.4	555.2	−106.0	−200.9
Lys	36.3	−26.5	−43.7	518.4	−101.2	−194.4
Met	30.1	−20.5	−38.4	510.1	−95.4	−193.5
Phe	50.6	−28.7	−50.9	536.2	−101.5	−198.2
Pro	71.9	−36.5	−59.4	573.6	−115.3	−200.5
Ser	9.3	−8.7	−11.7	589.1	−107.2	−193.8
Thr	11.5	−10.1	−14.6	379.8	−83.3	−156.7
Trp	79.4	−31.7	−66.1	596.7	−98.3	−210.3
Tyr	40.9	−23.2	−45.7	542.5	−96.3	−200.1
Val	42.3	−27.2	−44.8	501.0	−103.1	−196.3

From Eq. (22) and the data in Table IV, it is evident that there is always some degree of cancellation between the $E_{\rm relax}^{(2),e^-}$ and the $E_{e^-,e^+}^{(2),e^-,e^+}$ contributions to the binding energies, as the former is always negative and the latter always positive, according to the signs in Eq. (22). Since the loss in electron correlation tends to decrease the $\mathcal{E}_{\rm PBE}^{\rm HF}$ values, the APMO MP2 increment from APMO HF results arises for the e-p correlation contribution, which gives rise to a net increase in the PBEs. The average values of $E_{e^-,e^+}^{(2),e^-,e^+}$ in Table IV are 39.2 meV (HB) and 189.6 meV (ZW), being larger in absolute value than the $E_{\rm relax}^{(2),e^-}$ averages (in fact, the absolute values of $E_{e^-,e^+}^{(2),e^-,e^+}$ exceed those of $E_{\rm relax}^{(2),e^-}$ in all cases). Since the e-p correlation would be favored by the overlap between the electron and positron densities [3], the larger magnitude of the $E_{e^-,e^+}^{(2),e^-,e^+}$ term in the ZW structures, in comparison with the HB counterparts, indicates that the positron pulls the electron density away from the molecule more effectively in the ZW forms.

We now turn attention to the APMO P2 corrections to the APMO KT binding energies, defined as

$$\mathcal{E}_{\rm PBE}^{\rm P2} = \mathcal{E}_{\rm PBE}^{\rm KT} - \Sigma_{pp}^{e^+,e^-}\left(\omega_p^{e^+}\right), \tag{23}$$

which can be obtained from Eqs. (12)–(14). The self-energy $\Sigma_{pp}^{e^+,e^-}(\omega_p^{e^+})$, which accounts for the APMO P2 correction, can be decomposed into the pair-removal (PR) correlation, pair-relaxation, and orbital-relaxation (ORX) terms, following Ref. [44]. However, in the case of a molecular system containing multiple electrons and a single positron, the contributions

TABLE V. Decomposition of the APMO P2 level positron binding energies (in meV), according to Eq. (24). The results are shown for the 20 standard amino acids, indicated by the three-letter symbols, in the HB and ZW forms.

	HB			ZW		
Amino acid	$\mathcal{E}_{\rm PBE}^{\rm KT}$	$\mathcal{T}_{\rm ORX}$	$\mathcal{T}_{\rm PRM}$	$\mathcal{E}_{\rm PBE}^{\rm KT}$	$\mathcal{T}_{\rm ORX}$	$\mathcal{T}_{\rm PRM}$
Ala	64.3	−9.7	48.6	620.2	−74.3	206.2
Arg	87.3	−13.9	55.9	670.4	−85.8	215.4
Asn	20.4	−2.9	22.2	564.4	−73.1	199.7
Asp	21.8	−3.2	22.8	532.2	−68.8	189.8
Cys	18.7	−3.3	22.8	524.4	−72.9	191.5
Gln	58.3	−8.9	43.8	696.1	−86.7	218.4
Glu	76.6	−11.9	50.7	625.4	−79.6	206.6
Gly	67.8	−8.6	46.3	643.9	−67.1	200.6
His	4.2	−0.9	10.0	507.5	−76.9	193.5
Ile	63.1	−12.3	53.4	606.5	−89.1	218.7
Leu	73.9	−13.6	56.8	662.1	−88.7	222.3
Lys	48.5	−10.0	46.3	622	−84.1	214.9
Met	39.7	−8.2	40.5	613.4	−86.1	213.9
Phe	67.6	−14.3	54.2	650.7	−93.7	219.4
Pro	90.4	−15.3	63.4	678.5	−86.4	221.8
Ser	10.7	−1.2	12.1	681.9	−77.9	214.2
Thr	13.5	−1.7	15.2	453.9	−61.4	172.3
Trp	105.1	−22.5	70.8	723.2	−104.7	233.2
Tyr	55.6	−12.2	48.6	659.1	−94.9	221.5
Val	53.9	−10.0	47.4	603.8	−86.8	216.9

to the interparticle term reduce to

$$\Sigma_{pp}^{e^+e^-(2)}(\omega_p^{e^+}) = \sum_{a^{e^-}}^{O^{e^-}}\sum_{r^{e^-}}^{V^{e^-}}\sum_{r^{e^+}}^{V^{e^+}} \frac{|\langle p^{e^+}a^{e^-}|r^{e^+}r^{e^-}\rangle|^2}{\omega_p^{e^+}+\epsilon_a^{e^+}-\epsilon_r^{e^-}-\epsilon_r^{e^+}} + \sum_{a^{e^-}}^{O^{e^-}}\sum_{r^{e^-}}^{V^{e^-}}\sum_{a^{e^+}}^{O^{e^+}} \frac{|\langle p^{e^+}r^{e^-}|a^{e^+}a^{e^-}\rangle|^2}{\omega_p^{e^+}+\epsilon_r^{e^-}-\epsilon_a^{e^+}-\epsilon_a^{e^-}} = \mathcal{T}_{\rm PRM}+\mathcal{T}_{\rm ORX}, \quad (24)$$

where the PRM term $\mathcal{T}_{\rm PRM}$ is associated with the e-p correlation, while the ORX term $\mathcal{T}_{\rm ORX}$ is related to the electron relaxation upon positron detachment. These contributions for the HB and ZW structures are listed in Table V. It is clear that the negative $\mathcal{T}_{\rm ORX}$ values tend to decrease the binding energies and the positive PRM contributions tend to increase them. Similarly to APMO MP2, the contribution of the e-p correlation terms gives rise to a net increase of the $\mathcal{E}_{\rm PBE}^{\rm KT}$ values in all the cases since the $\mathcal{T}_{\rm PRM}$ terms have larger magnitudes.

Finally, we compare the performances of the APMO KT and APMO HF methods, as well as APMO MP2 and APMO P2. As shown in Table III, the APMO KT method predicts larger PBEs than the APMO HF. These higher binding energies result from the partial cancellation between the missing relaxation and correlation energies, which have opposite signs, in the APMO KT calculations. It is also clear in Table III that the APMO P2 method predicts larger PBEs than the APMO MP2. These discrepancies are related to the different basis sets employed in the calculations. The APMO MP2 binding energies are obtained from two basis sets, namely, one for the isolated molecule and another one for the positronic system. The APMO P2 calculations are in turn performed with a single basis set for the positronic problem. As discussed above, these differences generally favor the PBEs calculated with the APMO KT and APMO P2 methods with respect to those obtained at the APMO HF and APMO MP2 levels.

The computational effort associated with the APMO KT and APMO P2 methods is lower than those of the APMO HF and APMO MP2 methods, respectively. Both the $\mathcal{E}_{\rm PBE}^{\rm KT}$ and $\mathcal{E}_{\rm PBE}^{\rm P2}$ estimates are obtained from a single calculation for the positronic system, according to Eqs. (12) and (13), while the $\mathcal{E}_{\rm PBE}^{\rm HF}$ and $\mathcal{E}_{\rm PBE}^{\rm MP2}$ estimates are obtained from separate calculations for the isolated and positronic molecules, as indicated in Eq. (17). Moreover, the computational cost of the APMO P2 calculations scale as N_b^4, where N_b is the number of basis-set functions, while the APMO MP2 calculations scale as N_b^5. In summary, the calculated APMO KT binding energies are generally higher than the APMO HF counterparts, at half the computational cost. Similarly, calculated APMO P2 PBEs are generally higher than the APMO MP2 PBEs at a fraction of the computational cost.

V. CONCLUSION

We have devised a simple and computationally inexpensive procedure to select the best center for expanding the positron basis set, based on the condensed Fukui functions. It was also found that the choice for the expansion center can significantly impact the PBEs. We obtained PBEs for the 20 standard amino acids employing the APMO HF, APMO KT, APMO MP2, and APMO P2 levels of theory. In all cases, we considered GM, HB, and ZW structures. Our results indicated that APMO HF calculations generally provide lower bounds for the PBEs. These HF estimates can be generally increased with the inclusion of correlation in the APMO MP2 and APMO P2 schemes and it was also found that a cancellation of errors makes the APMO KT binding energies superior to those obtained at the APMO HF level. We have analyzed the origin of the differences in the calculated PBEs with the different methods and found that APMO MP2 and APMO P2 results are generally higher than the APMO HF results due to the predominance of the e-p correlation over relaxation in the PBEs. The PBEs obtained with the APMO KT and APMO MP2 methods have similar quality due to the cancellation of errors in the former, as mentioned above. Our results for these systems indicate that APMO KT and APMO P2 results are generally higher than APMO HF and APMO MP2 results. In addition, APMO KT and APMO P2 PBE calculations are more computationally efficient than their APMO HF and APMO MP2 counterparts. Our results suggest that APMO KT and APMO P2 methods are convenient options for the qualitative and semiquantitative analysis of the PBEs of medium- to large-size molecular systems.

In addition, since a number of relationships have been proposed to correlate positron binding energies and annihilation rates [3], we are currently deriving third-order MPBT expressions for calculating annihilation rates along the lines of Gribakin and Ludlow's work [67]. Annihilation rate results employing these expressions will be reported elsewhere.

ACKNOWLEDGMENTS

The authors acknowledge support from Fundação de Amparo à Pesquisa do Estado de São Paulo (Grants No. 2011/04986-2 and No. 2013/07712-6). M.T.d.N.V. also acknowledges support from Conselho Nacional de Desenvolvimento Científico e Tecnológico. J.R. acknowledges support from the Office of Research at Universidad Nacional (DIB Grant No. 201010020397).

[1] C. M. Surko, Nature (London) **449**, 153 (2007).
[2] J. Danielson, T. Weber, and C. M. Surko, in *Workshop on Cold Antimatter Plasmas and Applications to Fundaental Physics*, edited by Y. Kanai and Y. Yamazaki, AIP Conf. Proc. No. 1037 (AIP, New York, 2008), p. 84.
[3] G. Gribakin, J. Young, and C. M. Surko, Rev. Mod. Phys. **82**, 2557 (2010).
[4] M. Amoretti, C. Amsler, G. Bonomi, A. Bouchta, P. Bowe, C. Carraro, C. Cesar, M. Charlton, M. Collier, M. Doser *et al.*, Nature (London) **419**, 456 (2002).
[5] D. B. Cassidy and A. Mills, Nature (London) **449**, 195 (2007).
[6] S. Armitage, D. Leslie, J. Beale, and G. Laricchia, Nucl. Instrum. Methods Phys. Res. Sect. B **247**, 98 (2006).
[7] H. Walters, S. Sahoo, and S. Gilmore, Nucl. Instrum. Methods Phys. Res. Sect. B **233**, 78 (2005).
[8] J. R. Danielson, J. J. Gosselin, and C. M. Surko, Phys. Rev. Lett. **104**, 233201 (2010).
[9] P. M. Kozlowski and L. Adamowicz, J. Chem. Phys. **100**, 6266 (1996).
[10] K. Strasburger and H. Chojnacki, J. Chem. Phys. **108**, 3218 (1998).
[11] G. Ryzhikh, J. Mitroy, and K. Varga, J. Phys. B **31**, 3965 (1998).
[12] K. Strasburger, J. Chem. Phys. **111**, 10555 (1999).
[13] A. Chakraborty, M. V. Pak, and S. Hammes-Schiffer, J. Chem. Phys. **129**, 014101 (2008).
[14] D. M. Schrader, T. Yoshida, and K. Iguchi, Phys. Rev. Lett. **68**, 3281 (1992).
[15] T. Yoshida and G. Miyako, Phys. Rev. A **54**, 4571 (1996).
[16] D. Bressanini, M. Mella, and G. Morosi, J. Chem. Phys. **108**, 4756 (1998).
[17] M. Bromley, J. Mitroy, and G. Ryzhikh, Nucl. Instrum. Methods Phys. Res. Sect. B **171**, 47 (2000).
[18] M. Tachikawa, Chem. Phys. Lett. **360**, 494 (2002).
[19] M. Tachikawa, Chem. Phys. Lett. **350**, 269 (2001).
[20] J. Mitroy and M. W. J. Bromley, Phys. Rev. Lett. **98**, 063401 (2007).
[21] M. W. J. Bromley and J. Mitroy, Phys. Rev. A **75**, 042506 (2007).
[22] M. W. J. Bromley, J. Mitroy, and K. Varga, Phys. Rev. Lett. **109**, 063201 (2012).
[23] K. Strasburger and M. Wołcyrz, Mol. Phys. **105**, 467 (2007).
[24] K. Strasburger and M. Wolcyrz, Acta. Phys. Pol. A **113**, 1533 (2008).
[25] J. Mitroy and J. Y. Zhang, Phys. Rev. A **83**, 064701 (2011).
[26] R. J. Buenker, H.-P. Liebermann, V. Melnikov, M. Tachikawa, L. Pichl, and M. Kimura, J. Phys. Chem. A **109**, 5956 (2005).
[27] M. Tachikawa, Y. Kita, and R. J. Buenker, Phys. Chem. Chem. Phys. **13**, 2701 (2011).
[28] Y. Kita, R. Maezono, M. Tachikawa, M. D. Towler, and R. J. Needs, J. Chem. Phys. **135**, 054108 (2011).
[29] H. Chojnacki and K. Strasburger, Mol. Phys. **104**, 2273 (2006).
[30] K. Strasburger, Struct. Chem. **15**, 415 (2004).
[31] Y. Kita, R. Maezono, M. Tachikawa, M. Towler, and R. J. Needs, J. Chem. Phys. **131**, 134310 (2009).
[32] M. Tachikawa, K. Mori, H. Nakai, and K. Iguchi, Chem. Phys. Lett. **290**, 437 (1998).
[33] M. Tachikawa, K. Mori, K. Suzuki, and K. Iguchi, Int. J. Quantum Chem. **70**, 491 (1998).
[34] M. Ishida, M. Tachikawa, H. Tokiwa, K. Mori, and A. Ishii, Surf. Sci. **438**, 47 (1999).
[35] M. Tachikawa, R. J. Buenker, and M. Kimura, J. Chem. Phys. **119**, 5005 (2003).
[36] K. Koyanagi, Y. Kita, and M. Tachikawa, Eur. Phys. J. D **66**, 121 (2012).
[37] M. Kaneko, T. Udagawa, and M. Tachikawa, J. Comput. Chem. Jpn. **9**, 21 (2010).
[38] S. A. González, N. F. Aguirre, and A. Reyes, Int. J. Quantum Chem. **108**, 1742 (2008).
[39] F. Moncada, S. D. Cruz, and A. Reyes, Chem. Phys. Lett. **539-540**, 209 (2012).
[40] F. Moncada, S. D. Cruz, and A. Reyes, Chem. Phys. Lett. **570**, 16 (2013).
[41] F. Moncada, S. A. González, and A. Reyes, Mol. Phys. **108**, 1545 (2010).
[42] D. V. Moreno, S. A. González, and A. Reyes, J. Phys. Chem. A **114**, 9231 (2010).
[43] D. V. Moreno, S. A. González, and A. Reyes, J. Chem. Phys. **134**, 024115 (2011).
[44] J. Romero, E. F. Posada, R. Flores-Moreno, and A. Reyes, J. Chem. Phys. **137**, 074105 (2012).
[45] F. Moncada, E. F. Posada, R. Flores-Moreno, and A. Reyes, Chem. Phys. **400**, 103 (2012).
[46] R. Flores-Moreno, E. F. Posada, F. Moncada, J. Romero, J. Charry, M. Díaz-Tinoco, S. A. González, N. F. Aguirre, and A. Reyes, Int. J. Quantum Chem. **114**, 50 (2014).
[47] C. Makochekanwa, A. Bankovic, W. Tattersall, A. Jones, P. Caradonna, D. S. Slaughter, K. Nixon, M. J. Brunger, Z. Petrovic, J. P. Sullivan *et al.*, New J. Phys. **11**, 103036 (2009).
[48] A. Zecca, E. Trainotti, L. Chiari, G. García, F. Blanco, M. Bettega, M. d. N. Varella, M. Lima, and M. Brunger, J. Phys. B **44**, 195202 (2011).
[49] A. Zecca, E. Trainotti, L. Chiari, M. Bettega, S. d. Sanchez, M. d. N. Varella, M. Lima, and M. Brunger, J. Chem. Phys. **136**, 124305 (2012).
[50] L. Menichetti, L. Cionini, W. Sauerwein, S. Altieri, O. Solin, H. Minn, and P. Salvadori, Appl. Radiat. Isotopes **67**, S351 (2009).
[51] P. E. Valk, *Positron Emission Tomography: Basic Sciences* (Springer, Berlin, 2003).
[52] D. Donohue, L. Hulett, B. Eckenrode, S. McLuckey, and G. Glish, Chem. Phys. Lett. **168**, 37 (1990).
[53] L. Hulett, D. Donohue, J. Xu, T. Lewis, S. McLuckey, and G. Glish, Chem. Phys. Lett. **216**, 236 (1993).

[54] S. González and A. Reyes, Int. J. Quantum Chem. **110**, 689 (2010).
[55] M. Díaz-Tinoco, J. Romero, J. V. Ortiz, A. Reyes, and R. Flores-Moreno, J. Chem. Phys. **138**, 194108 (2013).
[56] P. K. Chattaraj, *Chemical Reactivity Theory: A Density Functional View* (CRC, Boca Raton, 2009).
[57] A. Szabó and N. S. Ostlund, *Modern Quantum Chemistry: Introduction To Advanced Electronic Structure Theory* (Dover, New York, 1996).
[58] In the physicist notation of quantum chemistry $\langle ab|cd\rangle = \int \psi_a^*(\mathbf{1})\psi_b^*(\mathbf{2})\psi_c(\mathbf{1})\psi_d(\mathbf{2})r_{12}^{-1}d\mathbf{r}_1 d\mathbf{r}_2$.
[59] See Supplemental Material at http://link.aps.org/supplemental/10.1103/PhysRevA.89.052709 for geometries of optimized GM, HB, and ZW amino-acid structures provided at the HF 6-311++G(d,p) level.
[60] J. Tomasi, B. Mennucci, and R. Cammi, Chem. Rev. **105**, 2999 (2005).
[61] M. Schmidt, K. Baldridge, J. Boatz, S. Elbert, M. Gordon, J. Jensen, S. Koseki, N. Matsunaga, K. Nguyen, S. Su, T. Windus, M. Dupuis, and J. Montgomery, J. Comput. Chem. **14**, 1347 (1993).
[62] C. M. Breneman and K. B. Wiberg, J. Comput. Chem. **11**, 361 (1990).
[63] O. Crawford, Proc. Phys. Soc. **91**, 279 (1967).
[64] P. Adamson, X. Duan, L. Burggraf, M. Pak, C. Swalina, and S. Hammes-Schiffer, J. Phys. Chem. A **112**, 1346 (2008).
[65] H. Abdoul-Carime and C. Desfrançois, Opt. Plasma Phys. **2**, 149 (1998).
[66] J. K. Pearson, P. M. Gill, J. M. Ugalde, and R. J. Boyd, Mol. Phys. **107**, 1089 (2009).
[67] G. F. Gribakin and J. Ludlow, Phys. Rev. A **70**, 032720 (2004).